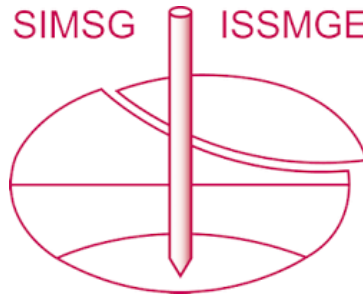


INTERNATIONAL SOCIETY FOR SOIL MECHANICS AND GEOTECHNICAL ENGINEERING



This paper was downloaded from the Online Library of the International Society for Soil Mechanics and Geotechnical Engineering (ISSMGE). The library is available here:

<https://www.issmge.org/publications/online-library>

This is an open-access database that archives thousands of papers published under the Auspices of the ISSMGE and maintained by the Innovation and Development Committee of ISSMGE.

The paper was published in the proceedings of the 7th International Conference on Earthquake Geotechnical Engineering and was edited by Francesco Silvestri, Nicola Moraci and Susanna Antonielli. The conference was held in Rome, Italy, 17 - 20 June 2019.

Seismic hazard analysis for tectonic earthquakes in the western area of Naples, Italy

H. Ebrahimiyan, F. Jalayer & G. Forte
University of Naples Federico II, Naples, Italy

V. Convertito
Istituto Nazionale di Geofisica e Vulcanologia (INGV), Osservatorio Vesuviano, Naples, Italy

V. Licata
Anas S.p.A, Rome, Italy

A. d'Onofrio, A. Santo & F. Silvestri
University of Naples Federico II, Naples, Italy

ABSTRACT: The Probabilistic Seismic Hazard Analysis (PSHA) is performed for the western area of the city Naples (southern Italy) by employing the database of individual seismogenic sources (DISS3.2) and parametric catalogue of Italian earthquakes (CPTI15). Seismogenic models include the individual seismogenic faults responsible for generating major earthquakes with magnitude greater than 5.5, and the background areal source model to encounter earthquakes with magnitude less than 5.5. In this context, the long-term earthquake recurrence on seismogenic tectonic faults as well as the spatial distribution of historical earthquakes are considered. Site amplifications are obtained from seismic microzonation maps derived for the designated area. Hazard maps are derived for a number of return periods for ground-shaking in terms of peak ground acceleration and 5%-damped pseudo-spectral acceleration at a range of periods that are representative of the existing construction within the area. Comparisons of the results with the code-based design spectra are provided.

1 INTRODUCTION

The reference seismic hazard map for Italy (Mappa di Pericolosità Sismica 2004, MPS04, Gruppo di Lavoro 2004a) was released by Istituto Nazionale di Geofisica e Vulcanologia (INGV) following the standard Cornell's PSHA approach (1968). The input parameters adopted by INGV for computing MPS04 were the CPTI04 earthquake catalog (Gruppo di Lavoro 2004b), the seismogenic source model ZS9 (Meletti et al. 2008), and the ground motion prediction equations (GMPEs) described in Montaldo et al. (2005). MPS04 provides the seismic hazard maps for Peak Ground Acceleration (*PGA*) with a probability of exceedance of 10% in 50 years. The MPS04 was consequently improved by carrying out the national research Project S1 (2004–2006, <http://esse1.mi.ingv.it/>). The project provided maps associated with different exceedance probabilities in 50 years for *PGA*, and the pseudo-spectral acceleration (*S_a*) at the period range of 0.1-2.0 seconds. The recent seismic sequences in central Italy raised the problem of seismogenic source characterization and seismicity rate estimation for faults that have been silent or unknown during historical times. The Database of Individual Seismogenic Sources (DISS) has been first developed in 2000 and updated in the next years (Basili et al. 2008). Nevertheless, the PSHA calculations in Italy (at national level) have not utilized so far the DISS data (Basili et al. 2008). These calculations are usually based on vast areal seismic source zones (e.g., Gruppo di Lavoro 2004a). However, the individual and composite seismogenic areas, recently introduced in the latest version 3.0 of the DISS

database (Basili et al. 2008) provide an interesting alternative to areal seismic zoning –to be explored in future Italian National seismic hazard maps.

The only seismic hazard maps available for the city of Naples in southern Italy are those provided by INGV in terms of MPS04 national hazard maps (not based on seismogenic individual faults). In this work, a new methodology has been implemented for carrying out site-specific PSHA for the western area of Naples. The seismogenic source modelling herein is based on a bi-layer model (Pace et al. 2006) including (a) the individual structures capable of producing major earthquakes (magnitude greater than 5.5), for which the magnitude recurrence relation and seismicity rate are estimated based on the DISS 3.2.0 subset data (DISS Working Group 2015); (b) background source model (magnitude less than 5.5) characterized based on the latest INGV-released catalogue of Italian earthquakes (CPTI15; Rovida et al. 2016, with events of magnitudes greater than or equal to 4.0 in the time period 1000-2014). The western area of Naples has a high potential of being affected by site response amplification, since it rests on soft soil of alluvial and volcanic origin. Herein, a detailed seismic microzonation has been conducted on the zone in order to properly evaluate the local soil-site effects. The seismic hazard maps for *PGA* and *Sa* at several periods (consistent with estimated first-mode vibration frequency for the building classes in this area) are provided (see Ebrahimian et al. 2018). Three most recent Italian, European and global models are adopted as GMPE's adopted herein; namely, ITA10 (Bindi et al. 2011), BND14 (Bindi et al. 2014a, b) and BSSA (Boore et al. 2014). Since ITA10 and BND14 use the geometric mean of the two horizontal components of ground motion, we have modified these two GMPEs in order to account for an arbitrary horizontal component of ground shaking. The seismic hazard results obtained in this study are compared (in terms of the uniform hazard spectrum and hazard curves) with the national hazard data provided by INGV and National Technical Code for seismic design (NTC 2018) for the designated site.

2 GEOLOGICAL CHARACTERISTICS AND MICROZONATION OF THE AREA

Fig. 1 shows the case-study area encompasses the zones of Bagnoli and Fuorigrotta (see the red-dashed rectangle and the yellow-highlighted area in the sub-figure). The area is an active volcanic field. Powerful eruptions in the past has led to the creation of geological formations (see the black and yellow-colored borders in the sub-figure of Fig. 1). The designated area rests on soft soil of alluvial and volcanic origin that can strongly affect the local seismic response. The urban fabric in this area consists of masonry and reinforced concrete constructions of different ages ranging from 1919 (and even older) up to 2001 (mainly constructed 1946-1971). Fig. 1 also shows the distribution of the composite seismic sources within and around the Campania region (Basili et al. 2008) together with few important historical events (highlighted with asterisks). The geological and geotechnical subsoil model adopted for the case-study area is described in detail in Licata et al. (2016) and Licata et al. (2019) and displayed in Fig. 2a as a synthetic geolithological map (see also Ebrahimian et al. 2018). The

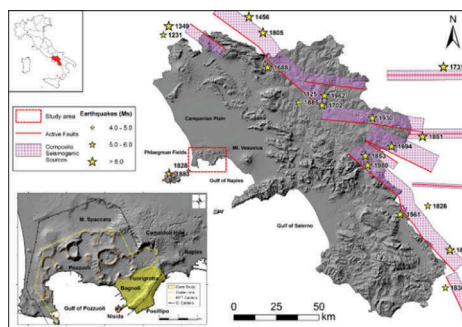


Figure 1. Tectonic and seismological setting of Campania Region; the location of the case-study area, main faults, and historical earthquakes

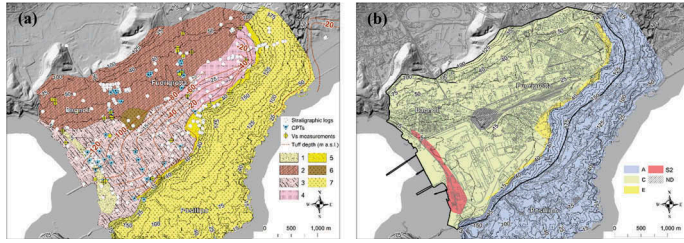


Figure 2. (a) Geolithological map of the area, (b) Seismic microzonation map

Table 1. Seismic Microzonation

Geological Characterization*	Soil Class**	V_{S30} (m/s)	Description
(1) Pyroclastic soils below sand dune	C	302	Aeolian sands above pyroclastic deposits made of clayey silts with peat layers, highly susceptible to liquefaction, classified as ground type S_2 in Fig. 2b
(2) Pyroclastic soils on un lithified NYT	C	295	Pyroclastic deposits lying on the soil of the NYT eruption. The depth of the bedrock is not defined.
(3) Pyroclastic and marine soils with peats on NYT	C	295	Pyroclastic deposits made of clayey silts with peat layers; the depth of the bedrock is $>20\text{m}$.
(4) Pyroclastic soils on NYT	C	295	Pyroclastic deposits made of clayey silts resting on the bedrock (NYT). The depth of the layer is $>20\text{m}$.
(5) Pyroclastic soils on NYT	E	196	Pyroclastic deposits made of clayey silts resting on the bedrock (NYT). The depth of the layer is $<20\text{m}$.
(6) Pyroclastic soils below STT	C	295	Pyroclastic deposits below the tuff of STT, characterized by V_S inversions. The class cannot be defined (ND); it is assumed to be of class C herein.
(7) NYT outcrop	A	800	Represents the engineering seismic bedrock of the whole area

* See the geological characterization map in Fig. 2a;

** See the site classification map in Fig. 2b.

black contour lines represent the topographic elevations. The seismic microzonation was carried out based on 30 measurements of the shear wave velocity (V_S) obtained through several geophysical tests. The locations of V_S -measurement tests are highlighted with yellow circles on Fig. 2a. Accordingly, the average shear wave velocity of the upper 30m, denoted as V_{S30} , is calculated for each geolithological complex. The seismic soil classification map, shown in Fig. 2b, is based on NTC (2008) site classes (Forte et al. 2017). The results of geological studies and microzonation of the area are summarized in Table 1 as follows:

3 SEISMOGENIC SOURCE CHARACTERIZATION

The first step in a PSHA procedure is the characterization of the seismogenic source model(s). The rectangular area located in southern Apennines, highlighted in Fig. 3a, is adopted herein as the “background area”. The Italian national seismogenic zones (ZS9, Gruppo di Lavoro 2004a) surrounding the background zone are also shown in Fig. 3a. Fig. 3b zooms in the background area, and the cyan-colored case-study area (i.e., the western part of the city of Naples) is shown also in Fig. 3b. The background area is extended from the case-study site through the northeast around 100 km and in the southeast direction around 160 km.

3.1 Finite-fault source models

The yellow-colored rectangles in Fig. 3b represent the Seismogenic Boxes (denoted herein as SBx) within the background area. As mentioned before, the SBx are the surface projection

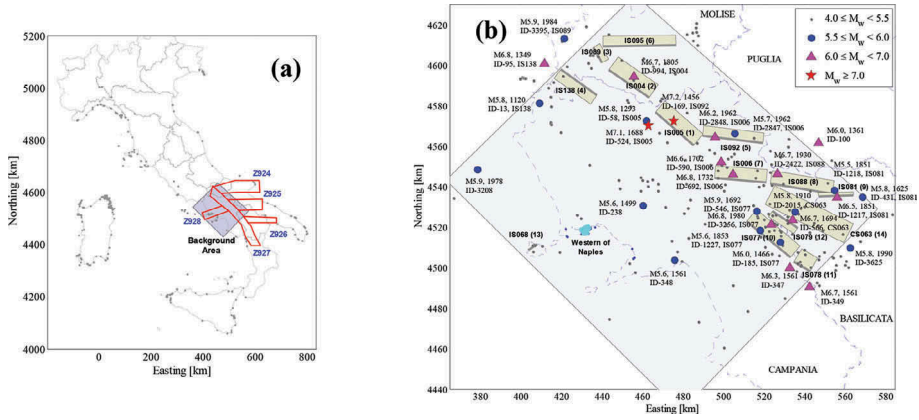


Figure 3. (a) the background area overlaid with the Italian seismic zonation (ZS9); (b) The 14 seismogenic sources within the background area

of individual seismogenic active faults. The name assigned by DISS 3.2.0 (DISS Working Group 2015) to each SBox is shown right next to the corresponding SBox, together with an identification (reference) number in the parenthesis. The closest edge of each seismic box to the ground surface is highlighted with thick gray line. The spatial distribution of historical earthquakes based on CPTI15 catalog in the time interval from 1000 to 2014 and with magnitude greater than 4.0 is also shown in Fig. 3b. For each event with $M_w \geq 5.5$ in Fig. 3b, two lines of information are provided: the first line specifies M_w and the time of occurrence (year) of the event; the second line identifies the record's label in CPTI15 catalog and the seismogenic fault to which it is attributed (if available). A complete description of these SBox's together with the historical earthquake(s) assigned to each SBox is summarized in Ebrahimian et al. (2018).

To estimate the distribution of maximum characteristic magnitude on a fault segment, five different methods are employed herein (see Ebrahimian et al. 2018 for the complete description of each method). The vector of alternative calculated/observed maximum moment magnitude estimates (based on five different methods), denoted as \mathbf{M}_{\max} , and the corresponding dispersions, $\sigma_{\mathbf{M}_{\max}}$, are considered for characterizing the distribution of the maximum characteristic magnitude. In this context, M_{char} denotes the average value of the maximum magnitude and σ_m represents its standard deviation. Thus,

$$M_{\text{char}} = \overline{\mathbf{M}_{\max}}, \quad \sigma_m = \sqrt{s_{\mathbf{M}_{\max}}^2 + \frac{1}{n_{\mathbf{M}_{\max}}} \sum_{i=1}^{n_{\mathbf{M}_{\max}}} \sigma_{\mathbf{M}_{\max}(i)}^2} \quad (1)$$

where $\overline{\mathbf{M}_{\max}}$ is the average of the vector \mathbf{M}_{\max} , $n_{\mathbf{M}_{\max}} = 5$ is the length of the vector \mathbf{M}_{\max} , $s_{\mathbf{M}_{\max}}$ is the sample standard deviation of the calculated/observed values in \mathbf{M}_{\max} , and finally $\sigma_{\mathbf{M}_{\max}(i)}$ is the standard deviation reported for each individual component in \mathbf{M}_{\max} . Note that the expression in Eq. (1) encompasses not only the uncertainty in the estimation of $\overline{\mathbf{M}_{\max}}$, but also the dispersion due to the calculated/observed values in \mathbf{M}_{\max} . Eq. (1) is derived assuming that the different components of \mathbf{M}_{\max} are uncorrelated. A truncated normal probability density function with M_{char} as mean and σ_m as the standard deviation can be generated for each SBox. The normal distribution is truncated at a lower magnitude equal to $M_l^{\text{SB}} = 5.50$ in one side and at an upper magnitude M_u^{SB} lying two standard deviation above the mean value, $M_{\text{char}} + 2\sigma_m$ (for the upper-bound truncation). This truncated PDF, denoted herein as f_M^{SB} , can then be expressed as,

$$f_M^{\text{SB}}(m) = \phi\left(\frac{m - M_{\text{char}}}{\sigma_m}\right) / \left(\Phi\left(\frac{M_u^{\text{SB}} - M_{\text{char}}}{\sigma_m}\right) - \Phi\left(\frac{M_l^{\text{SB}} - M_{\text{char}}}{\sigma_m}\right) \right) \quad (2)$$

where $\phi(\cdot)$ is the standard Normal PDF, and $\Phi(\cdot)$ is the standard Normal cumulative density function (CDF).

The activity rate can be expressed in terms of mean annual rate of events with magnitude greater than or equal to $M_l^{SB}=5.50$ for each SBox. The annual seismicity rate to each seismic box, denoted as ν^{SB} , is assumed herein to be the maximum value obtained by employing three different methods (see Ebrahimian et al. 2018). The first method uses the geometric and kinematic parameters assigned to each SBox based on the conservation of seismic moment; the second method estimates the mean occurrence time of the characteristic magnitude, T_{mean} , assigned to each SBox (Peruzza et al. 2010) using the criterion of segment seismic moment conservation; finally, a rough estimate for the seismicity rate can be calculated as the number of events with $M > M_l^{SB}$ divided by the time span.

3.2 Background source model

The magnitude distribution for the background source, denoted as f_M^{BG} follows a truncated Exponential distribution as (see also Jalayer et al. 2011, Ebrahimian et al. 2014):

$$f_M^{BG}(m) = \frac{\beta e^{-\beta m}}{e^{-\beta M_l^{BG}} - e^{-\beta M_l^{SB}}} \quad (3)$$

where $M_l^{BG} \leq m \leq M_l^{SB}=5.50$, M_l^{BG} is the lower cut-off magnitude of the background area, β is the slope of the Gutenberg-Richter (GR) earthquake rate model. The first step toward quantifying f_M^{BG} is to have an estimate of M_l^{BG} . The designated lower cut-off magnitude of the background area M_l^{BG} should be greater than or equal to M_c , i.e., $M_l^{BG} \geq M_c$, where M_c denotes the completeness magnitude. To find M_c , we have employed two different methods (see Ebrahimian et al. 2018): direct use of frequency-magnitude distribution plot, and Bayesian updating approach for calculating the β -value versus various magnitude thresholds (see also Ebrahimian et al. 2014; Ebrahimian and Jalayer 2017). Accordingly, we set $M_l^{BG}=4.60$. The next parameters required are β (for calculating f_M^{BG}) and also the seismicity rate.

To make a sound estimate of the seismicity rate, it is essential to identify a time interval in which the catalogue is complete, known as the *completeness interval*. More specifically, the completeness interval is the time interval in which the magnitude range assigned to the background, i.e., $M_l^{BG}=4.60 \leq m \leq M_l^{SB}=5.50$, is likely to be completely reported. In this study, we use two different methods to address this issue (see Ebrahimian et al. 2018): (a) the *Visual Cumulative Method* proposed by and Mulargia et al. (1987); and (b) the statistical approach called herein as *Stepp Method* and proposed by Stepp (1972). According to both methods, the time interval of [1900-2014] is considered as the completeness period of the catalog for the desired background area. As a result, one can estimate the annual rate of events within the background area as $\nu(M_l^{BG} \leq M \leq M_l^{SB}) \triangleq \nu^{BG} = 0.37$. To find the GR seismicity slope β , the Bayesian updating approach described previously is used which gives the maximum likelihood (mode) of the posterior distribution of β at 2.83. This value is used for estimating f_M^{BG} in Eq. (3).

3.3 The ground motion prediction models

A GMPE represents the probability distribution for a given ground shaking parameter at a designated site as a function of source/site characteristics such as magnitude, source-to-site distance, style of faulting, and soil-site conditions. The GMPEs selected for this study are as follows: (a) ITA10 (Bindi et al. 2011) derived based on the improved seismic Italian archive (ITACA; <http://itaca.mi.ingv.it>), with site classification based on national code (NTC 2018); (b) BND14 (Bindi et al. 2014a, b) derived from the reference database for seismic ground-motion prediction in Europe with site classification based on NTC as well as V_{S30} (i.e., measured average shear-wave velocity of the uppermost 30 m of the soil layer); (c) and BSSA (Boore et al. 2014) derived from the PEER NGA-West2 database and site classification based on V_{S30} (see also Ebrahimian et al. 2019). While ITA10 and BND14 use geometric mean of the two horizontal components of ground motion., BSSA employs the single-component horizontal ground-motion. Integrating seismic hazard calculated based on the GMPE with geometric mean of the two horizontal

components of ground-motion, and structural analysis based on single-component horizontal ground-motion, leads to inaccurate and unconservative estimates of the seismic risk. To overcome this inconsistency in GMPEs, the ITA10 and BND14 are modified herein in order to account also for the arbitrary component of ground shaking (see Ebrahimian et al. 2019 for more details).

4 PROBABILISTIC SEISMIC HAZARD ASSESSMENT

Probabilistic seismic hazard analysis (PSHA) is the most appropriate approach for considering various sources of uncertainty to be explicitly considered for the evaluation of seismic hazard. The annual rate of exceeding a specified level of ground-motion intensity measure, IM , equal to x is denoted as $\lambda(IM > x)$. The rate $\lambda(IM > x)$ can be expressed as the sum of the exceedance rates for all seismic sources including: (a) finite-fault sources (a.k.a. SB $_{i}$'s and denoted as SB $_{i}$, where $i=1, \dots, n_{SB}=14$, see Fig. 3b); (b) areal source (i.e., background, denoted as BG). Thus, the rate $\lambda(IM > x)$ can be calculated as follows:

$$\lambda(IM > x) = \sum_{i=1}^{n_{SB}} \lambda_{SB_i}(IM > x) + \lambda_{BG}(IM > x) \quad (4)$$

By employing the concept of filtered Poisson, one can express Eq. (4) as:

$$\lambda(IM > x) = \sum_{i=1}^{n_{SB}} \underbrace{\lambda_{SB_i}(M > M_i^{SB})}_{\nu_{SB_i}} \cdot P(IM > x | EQ_{SB_i}) + \underbrace{\lambda_{BG}(M_i^{SB} \geq M \geq M_i^{BG})}_{\nu_{BG}} \cdot P(IM > x | EQ_{BG}) \quad (5)$$

The terms $P(IM > x | EQ_{SB_i})$ and $P(IM > x | EQ_{BG})$ denote the probability of $IM > x$ given that an EQ of interest takes place in SB $_{i}$ and BG, respectively. These exceedance probabilities are described by a lognormal distribution whose statistical parameters (logarithmic mean and standard deviation) are provided by a prescribed GMPE taking into account the joint probability distribution for the model parameters θ , denoted as $f(\theta)$. By using total probability theorem, and assuming that Ω_{θ} is the domain of the model parameters θ , Eq. (5) can be re-written as:

$$\lambda(IM > x) = \sum_{i=1}^{n_{SB}} \nu_{SB_i} \int_{\Omega_{\theta_{SB_i}}} P(IM > x | EQ_{SB_i}, \theta_{SB_i}) f(\theta_{SB_i}) d\theta_{SB_i} + \nu_{BG} \int_{\Omega_{\theta_{BG}}} P(IM > x | EQ_{BG}, \theta_{BG}) f(\theta_{BG}) d\theta_{BG} \quad (6)$$

The model parameters θ_{SB} and θ_{BG} for finite fault sources and the background area are described in details in Ebrahimian et al. (2018).

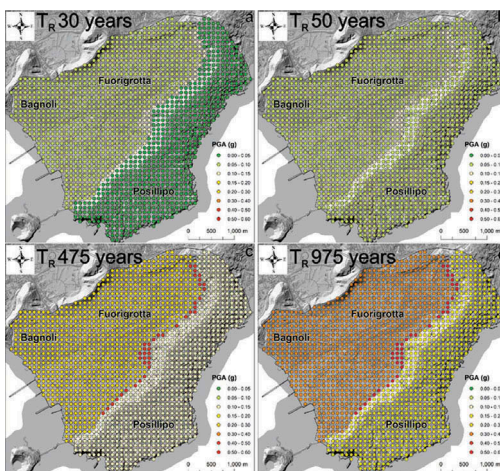


Figure 4. Seismic Hazard maps for PGA for the return periods of [30, 50, 475, 975] years

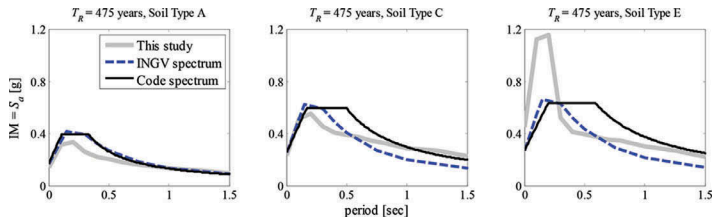


Figure 5. Comparison of the UHS of this study with the INGV-based and code-based spectra

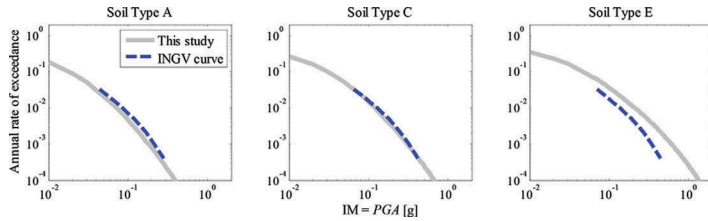


Figure 6. Comparison of the PSHA curves estimated by this study with the INGV curves

4.1 The seismic hazard analysis maps

The site-specific seismic hazard maps are extracted from the seismic hazard curves calculated for a grid of sites covering the studied area. Herein, we demonstrate the seismic hazard maps calculated for PGA corresponding to four hazard levels with T_R (inverse of mean annual rate of exceedance) of [30, 50, 475, 975] years in Fig. 4 (for more IMs , see Ebrahimian et al. 2018).

The PSHA estimates in terms of Uniform Hazard Spectrum (UHS, a by-product of site-specific PSHA that expresses S_a values for a range of periods given a uniform hazard level) are compared with the national hazard map data (<http://esse1.mi.ingv.it/>) released by INGV as well as the code-based response spectra (NTC 2018). The UHS estimated by this study are shown for one hazard level in Fig. 5 together with the INGV-based spectra (for the nearest grid point) and the code-based spectra (NTC 2018). It is to note that the INGV spectra are derived for stiff-soil condition (i.e., soil type A) and they should be later modified for site amplification effects.

The UHS is also a by-product of the PSHA that is useful especially in the seismic probabilistic assessment of building structures (Ebrahimian et al. 2014, Jalayer and Cornell 2009, Jalayer et al. 2017). To this end, the PSHA curves constructed by this study for a reference points are compared with the INGV hazard curves (<http://esse1.mi.ingv.it/>) in Fig. 6.

5 SUMMARY AND CONCLUSIONS

A Probabilistic seismic hazard analysis (PSHA) is performed for the western area of the city Naples (southern Italy) based on a bi-layer model of seismogenic tectonic faults, together with the background spatial model. The site amplification is seen through a detailed seismic microzonation study derived for the area. PSHA maps are presented for a number of return periods (corresponding to prescribed probability of exceedance in 50 years) for peak ground acceleration (PGA). By comparing the seismic hazard results obtained in this study with the national hazard maps provided by INGV and the national Italian code (NTC 2018), the following observations are made: (1) The seismic intensities suggested by INGV for $T > 0.5$ sec are underestimated for medium-to-soft soil sites compared to the study performed herein. (2) The UHS for $T < 0.50$ sec is considerably underestimated both by INGV and national

code for soft soil type E. (3) For soft soil sites (soil types C and E), INGV-based hazard curves underestimate the annual exceedance frequencies for *PGA* compared to our study. (4) More attention needs to be focused on the consideration of local amplification on soft soil (especially soil type E).

ACKNOWLEDGEMENT

This work was supported in part by Project METROPOLIS (**Met**odologie e **Tecnologie** Integrate e **Sostenibili** Per L'adattamento e **La Sicurezza** di Sistemi Urbani). This support is gratefully acknowledged.

REFERENCES

- Basili R, Valensise G, Vannoli P, Burrato P, Fracassi U, Mariano S, Tiberti MM, Boschi E (2008) The Database of Individual Seismogenic Sources (DISS), version 3: summarizing 20 years of research on Italy's earthquake geology. *Tectonophysics* 453:20–43. doi: 10.1016/j.tecto.2007.04.014.
- Bindi D, Pacor F, Luzi L, Puglia R, Massa M, Ameri G, Paolucci R (2011) Ground motion prediction equations derived from the Italian strong motion database. *Bull Earthq Eng*, 9(6):1899–1920.
- Bindi D, Massa M, Luzi L, Ameri G, Pacor F, Puglia R, Augliera P (2014a) Pan-European ground-motion prediction equations for the average horizontal component of PGA, PGV, and 5%-damped PSA at spectral periods up to 3.0 s using the RESORCE dataset. *Bull Earthq Eng* 12(1):391–430.
- Bindi D, Massa M, Luzi L, Ameri G, Pacor F, Puglia R, Augliera P (2014b) Erratum to: Pan-European ground-motion prediction equations for the average horizontal component of PGA, PGV, and 5%-damped PSA at spectral periods up to 3.0 s using the RESORCE dataset. *Bull Earthq Eng* 12(1): 431–448.
- Boore DM, Stewart JP, Seyhan E, Atkinson GM (2014) NGA-West2 equations for predicting PGA, PGV, and 5% damped PSA for shallow crustal earthquakes. *Earthq Spectra*, 30(3): 1057–1085.
- Cornell CA (1968) Engineering seismic risk analysis. *Bull Seismol Soc Am*, 58 (5):1583–1606.
- DISS Working Group (2015) Database of Individual Seismogenic Sources (DISS), Version 3.2.0: A compilation of potential sources for earthquakes larger than M 5.5 in Italy and surrounding areas. *Istituto Nazionale di Geofisica e Vulcanologia*; doi: 10.6092/INGV.IT-DISS3.2.0.
- Ebrahimian H, Azarbakht AR, Tabandeh A, Golafshani AA (2012) The exact and approximate conditional spectra in the multi-seismic-sources regions. *Soil Dyn Earthq Eng* 39 (1): 61–77.
- Ebrahimian H, Jalayer F, Asprone D, Lombardi AM, Marzocchi W, Prota A, Manfredi G. (2014) Adaptive daily forecasting of seismic aftershock hazard. *Bull. Seism. Soc. Am.*, 104 (1): 145–161.
- Ebrahimian H, Jalayer F (2017) Robust seismicity forecasting based on Bayesian parameter estimation for epidemiological spatio-temporal aftershock clustering models. *Scientific Reports*, Nature, 7(9803): 1–15. doi: 10.1038/s41598-017-09962-z.
- Ebrahimian H, Jalayer F, Forte G., Convertito V., Licata V., d'Onofrio A., Santo A., Silvestri F., Manfredi G. (2019) Site-specific probabilistic seismic hazard analysis for the Western area of Naples, Italy. *Bull Earthq Eng* (Under Review)
- Forte G, Fabbrocino S, Fabbrocino G, Lanzano G, Santucci de Magistris F, Silvestri F (2017). A geolithological approach to seismic site classification: an application to the Molise Region (Italy). *Bull Earthquake Eng*, 15 (1): 175–198.
- Gruppo di Lavoro (2004a). *Redazione della mappa di pericolosità sismica prevista dall'Ordinanza PCM 3274 del 20 marzo 2003*. Rapporto Conclusivo per il Dipartimento della Protezione Civile, INGV, Milano-Roma, April 2004: 65 pp. + 5 appendixes (in Italian).
- Gruppo di lavoro CPTI (2004b). *Catalogo Parametrico dei Terremoti Italiani, versione 2004 (CPTI04)*, INGV, Bologna. DOI: <http://doi.org/10.6092/INGV.IT-CPTI04>.
- Jalayer F, Cornell CA (2009) Alternative non-linear demand estimation methods for probability-based seismic assessments. *Earthq Eng Struct Dyn*, 38 (8): 951–972.
- Jalayer F, Asprone D, Prota A, Manfredi G (2011) A decision support system for post-earthquake reliability assessment of structures subjected to aftershocks: an application to L'Aquila earthquake, 2009. *Bull Earthq Eng*, 9 (4): 997–1014.
- Jalayer F, Ebrahimian H, Miano A, Manfredi G, Sezen H (2017) Analytical fragility assessment using un-scaled ground motion records. *Earthq Eng Struct Dyn*, 46(15): 2639–2663. DOI: 10.1002/eqe.2922.
- Licata V, Forte G, d'Onofrio A, Evangelista L, Jalayer F, Santo A, Silvestri F. (2016). Microzonation Study on the Western area of Napoli. *Procedia Engineering*, 158: 511–516.

- Licata V, Forte G, d'Onofrio A, Santo A, Silvestri F (2019). A multi-level study for the seismic microzonation of the Western area of Napoli (Italy). *Bull Earthq Eng* (under review).
- Meletti C, Galadini F, Valensise G, Stucchi M, Basili R, Barba G, Vannucci G, Boschi E (2008) A seismic source model for the seismic hazard assessment of the Italian territory. *Tectonophysics* 450(1): 85–108.
- Montaldo, V, Faccioli E, Zonno G, Akinci A, Malagnini L (2005) Treatment of ground-motion predictive relationships for the reference seismic hazard map of Italy. *J Seismol* 9(3): 295–316.
- Mulargia F, Gasperini P, Tinti S (1987) Contour mapping of Italian seismicity. *Tectonophysics* 142: 203–216.
- NTC (2018). *Aggiornamento delle «Norme tecniche per le costruzioni»*. Gazzetta Ufficiale 42, 20 February 2018.
- Pace B, Peruzza L, Lavecchia G, Boncio P (2006). Layered seismogenic source model and probabilistic seismic-hazard analyses in central Italy. *Bull. Seismol. Soc. Am.* 96 (1): 107–132.
- Peruzza L, Pace B, Cavallini F (2010) Error propagation in time-dependent probability of occurrence for characteristic earthquakes in Italy. *J Seismol* 14 (1): 119–141.
- Rovida A, Locati M, Camassi R, Lolli B, Gasperini P (eds) (2016). *CPTI15, the 2015 version of the Parametric Catalogue of Italian Earthquakes*. Istituto Nazionale di Geofisica e Vulcanologia.
- Stepp JC (1972) Analysis of completeness of the earthquake sample in the Puget Sound area and its effect on statistical estimates of earthquake hazard. In: Proceedings of first microzonation conference, Seattle, USA, pp 897–909.